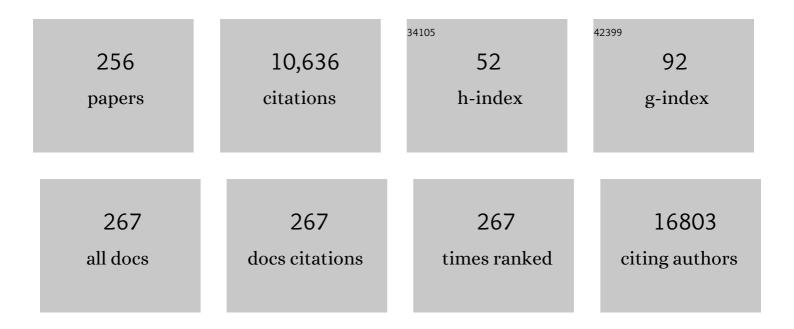
List of Publications by Year in descending order

Source: https://exaly.com/author-pdf/2279778/publications.pdf Version: 2024-02-01



HAIDIN SU

#	Article	IF	CITATIONS
1	Phosphorene: from theory to applications. Nature Reviews Materials, 2016, 1, .	48.7	815
2	A stable solution-processed polymer semiconductor with record high-mobility for printed transistors. Scientific Reports, 2012, 2, 754.	3.3	800
3	Tuning the crystal morphology and size of zeolitic imidazolate framework-8 in aqueous solution by surfactants. CrystEngComm, 2011, 13, 6937.	2.6	371
4	Pits confined in ultrathin cerium(IV) oxide for studying catalytic centers in carbon monoxide oxidation. Nature Communications, 2013, 4, 2899.	12.8	326
5	Catalysis mechanisms of CO ₂ and CO methanation. Catalysis Science and Technology, 2016, 6, 4048-4058.	4.1	316
6	CO ₂ Electroreduction Performance of Transition Metal Dimers Supported on Graphene: A Theoretical Study. ACS Catalysis, 2015, 5, 6658-6664.	11.2	227
7	Pseudo-topotactic conversion of carbon nanotubes to T-carbon nanowires under picosecond laser irradiation in methanol. Nature Communications, 2017, 8, 683.	12.8	184
8	Strain effect on electronic structures of graphene nanoribbons: A first-principles study. Journal of Chemical Physics, 2008, 129, 074704.	3.0	182
9	Tuning the electronic structure of graphene nanoribbons through chemical edge modification: A theoretical study. Physical Review B, 2007, 75, .	3.2	156
10	Single-Crystalline, Ultrathin ZnGa ₂ O ₄ Nanosheet Scaffolds To Promote Photocatalytic Activity in CO ₂ Reduction into Methane. ACS Applied Materials & Interfaces, 2014, 6, 2356-2361.	8.0	151
11	Insight into Proton Transfer in Phosphotungstic Acid Functionalized Mesoporous Silica-Based Proton Exchange Membrane Fuel Cells. Journal of the American Chemical Society, 2014, 136, 4954-4964.	13.7	147
12	Newly Developed Stepwise Electroless Deposition Enables a Remarkably Facile Synthesis of Highly Active and Stable Amorphous Pd Nanoparticle Electrocatalysts for Oxygen Reduction Reaction. Journal of the American Chemical Society, 2014, 136, 5217-5220.	13.7	132
13	Elucidating the role of disorder and free-carrier recombination kinetics in CH3NH3PbI3 perovskite films. Nature Communications, 2015, 6, 7903.	12.8	132
14	Room Temperature Synthesis of Stable, Printable Cs ₃ Cu ₂ X ₅ (X = I,) Tj ET Chemistry of Materials, 2020, 32, 5515-5524.	Qq0 0 0 r 6.7	gBT /Overlock 127
15	Automated Derivation of Bathymetric Information from Multi-Spectral Satellite Imagery Using a Non-Linear Inversion Model. Marine Geodesy, 2008, 31, 281-298.	2.0	115
16	Curvature-Dependent Selectivity of CO ₂ Electrocatalytic Reduction on Cobalt Porphyrin Nanotubes. ACS Catalysis, 2016, 6, 6294-6301.	11.2	113
17	Highly Efficient Chemical Process To Convert Mucic Acid into Adipic Acid and DFT Studies of the Mechanism of the Rhenium atalyzed Deoxydehydration. Angewandte Chemie - International Edition, 2014, 53, 4200-4204.	13.8	112
18	Textured fluorapatite bonded to calcium sulphate strengthen stomatopod raptorial appendages. Nature Communications, 2014, 5, 3187.	12.8	103

HAIBIN SU

#	Article	IF	CITATIONS
19	Half-Metallicity in Organic Single Porous Sheets. Journal of the American Chemical Society, 2012, 134, 5718-5721.	13.7	101
20	"Clean Reaction―Strategy to Approach a Stable, Green Heptatwistacene Containing a Single Terminal Pyrene Unit. Chemistry - an Asian Journal, 2012, 7, 672-675.	3.3	98
21	Computed and Experimental Absorption Spectra of the Perovskite CH ₃ NH ₃ PbI ₃ . Journal of Physical Chemistry Letters, 2014, 5, 3061-3065.	4.6	94
22	Anisotropic Electronic Characteristics, Adsorption, and Stability of Low-Index BiVO ₄ Surfaces for Photoelectrochemical Applications. ACS Applied Materials & Interfaces, 2018, 10, 5475-5484.	8.0	93
23	Theoretical Modelling and Facile Synthesis of a Highly Active Boronâ€Doped Palladium Catalyst for the Oxygen Reduction Reaction. Angewandte Chemie - International Edition, 2016, 55, 6842-6847.	13.8	92
24	Comparison of satellite reflectance algorithms for estimating chlorophyll-a in a temperate reservoir using coincident hyperspectral aircraft imagery and dense coincident surface observations. Remote Sensing of Environment, 2016, 178, 15-30.	11.0	92
25	Theoretical Insight into the Mechanism of Photoelectrochemical Oxygen Evolution Reaction on BiVO ₄ Anode with Oxygen Vacancy. Journal of Physical Chemistry C, 2017, 121, 18702-18709.	3.1	89
26	Bonding Pathways of Gold Nanocrystals in Solution. Nano Letters, 2014, 14, 6639-6643.	9.1	87
27	Magnetic ions in wide band gap semiconductor nanocrystals for optimized thermoelectric properties. Materials Horizons, 2014, 1, 81-86.	12.2	87
28	Persistently Folded Circular Aromatic Amide Pentamers Containing Modularly Tunable Cation-Binding Cavities with High Ion Selectivity. Journal of the American Chemical Society, 2010, 132, 9564-9566.	13.7	86
29	A Pilot Study of Mesenchymal Stem Cell Therapy for Acute Liver Allograft Rejection. Stem Cells Translational Medicine, 2017, 6, 2053-2061.	3.3	86
30	Density functional theory and molecular dynamics studies of the energetics and kinetics of electroactive polymers: PVDF and P(VDF-TrFE). Physical Review B, 2004, 70, .	3.2	82
31	Arene CHO Hydrogen Bonding: A Stereocontrolling Tool in Palladiumâ€Catalyzed Arylation and Vinylation of Ketones. Angewandte Chemie - International Edition, 2013, 52, 4906-4911.	13.8	82
32	Electronic and magnetic properties of V-doped anataseTiO2from first principles. Physical Review B, 2006, 74, .	3.2	80
33	Optical fiber magnetic field sensor based on magnetic fluid and microfiber mode interferometer. Optics Communications, 2015, 336, 5-8.	2.1	80
34	Synthesis, Structural Investigations, Hydrogenâ^'Deuterium Exchange Studies, and Molecular Modeling of Conformationally Stablilized Aromatic Oligoamides. Journal of the American Chemical Society, 2010, 132, 5869-5879.	13.7	79
35	Density functional theory based screening of ternary alkali-transition metal borohydrides: A computational material design project. Journal of Chemical Physics, 2009, 131, 014101.	3.0	77
36	Five-Fold-Symmetric Macrocyclic Aromatic Pentamers: High-Affinity Cation Recognition, Ion-Pair-Induced Columnar Stacking, and Nanofibrillation. Journal of the American Chemical Society, 2011, 133, 13930-13933.	13.7	77

#	Article	IF	CITATIONS
37	Crystallographic Evidence of an Unusual, Pentagon-Shaped Folding Pattern in a Circular Aromatic Pentamer. Organic Letters, 2008, 10, 5127-5130.	4.6	74
38	Terahertz Conductivity of Twisted Bilayer Graphene. Physical Review Letters, 2013, 110, 067401.	7.8	73
39	Intensity-modulated magnetic field sensor based on magnetic fluid and optical fiber gratings. Applied Physics Letters, 2013, 103, 183511.	3.3	68
40	Scaling of Excitons in Graphene Nanoribbons with Armchair Shaped Edges. Journal of Physical Chemistry A, 2011, 115, 11998-12003.	2.5	61
41	Crystallographic Realization of the Mathematically Predicted Densest Allâ€Pentagon Packing Lattice by <i>C</i> ₅ ymmetric "Sticky―Fluoropentamers. Angewandte Chemie - International Edition, 2011, 50, 10612-10615.	13.8	61
42	Merging of metal nanoparticles driven by selective wettability of silver nanostructures. Nature Communications, 2014, 5, 2994.	12.8	61
43	A Facile Strategy To Prepare Smart Coatings with Autonomous Self-Healing and Self-Reporting Functions. ACS Applied Materials & amp; Interfaces, 2020, 12, 4870-4877.	8.0	61
44	Combination Therapy Strategy of Quorum Quenching Enzyme and Quorum Sensing Inhibitor in Suppressing Multiple Quorum Sensing Pathways of P. aeruginosa. Scientific Reports, 2018, 8, 1155.	3.3	60
45	Graphene-based spin logic gates. Applied Physics Letters, 2011, 98, .	3.3	59
46	Geographically Adaptive Inversion Model for Improving Bathymetric Retrieval From Satellite Multispectral Imagery. IEEE Transactions on Geoscience and Remote Sensing, 2014, 52, 465-476.	6.3	59
47	An enzyme mimic ammonium polymer as a single catalyst for glucose dehydration to 5-hydroxymethylfurfural. Green Chemistry, 2015, 17, 2348-2352.	9.0	59
48	Iron-phthalocyanine molecular junction with high spin filter efficiency and negative differential resistance. Journal of Chemical Physics, 2012, 136, 064707.	3.0	58
49	Helical Organization in Foldable Aromatic Oligoamides by a Continuous Hydrogen-Bonding Network. Organic Letters, 2009, 11, 1201-1204.	4.6	57
50	Average density of states in disordered graphene systems. Physical Review B, 2008, 77, .	3.2	54
51	Self-sorting heterodimeric coiled coil peptides with defined and tuneable self-assembly properties. Scientific Reports, 2015, 5, 14063.	3.3	54
52	Deriving Bathymetry From Optical Images With a Localized Neural Network Algorithm. IEEE Transactions on Geoscience and Remote Sensing, 2018, 56, 5334-5342.	6.3	54
53	Excitonic Photoluminescence from Nanodisc States in Graphene Oxides. Journal of Physical Chemistry Letters, 2014, 5, 1754-1759.	4.6	53
54	Chiral crystallization of aromatic helical foldamers via complementarities in shape and end functionalities. Chemical Science, 2012, 3, 2042.	7.4	52

#	Article	IF	CITATIONS
55	Quantum confinement-induced tunable exciton states in graphene oxide. Scientific Reports, 2013, 3, 2250.	3.3	52
56	Encapsulation of Conventional and Unconventional Water Dimers by Water-Binding Foldamers. Organic Letters, 2011, 13, 3194-3197.	4.6	51
57	Transport properties of HfO <mml:math <br="" xmlns:mml="http://www.w3.org/1998/Math/MathML">display="inline"><mml:msub><mml:mrow /><mml:mrow><mml:mn>2</mml:mn><mml:mo>â[°]</mml:mo><mml:mi>x</mml:mi></mml:mrow></mml:mrow </mml:msub> resistive-switching memories. Physical Review B. 2012. 85.</mml:math>	< ³m ml:ma	ıtĥ∮based
58	Molecular Insights into Smallâ€Molecule Drug Discovery for SARSâ€CoVâ€2. Angewandte Chemie - International Edition, 2021, 60, 9789-9802.	13.8	50
59	Observation of room-temperature high-energy resonant excitonic effects in graphene. Physical Review B, 2011, 84, .	3.2	48
60	Dynamic friction force in a carbon peapod oscillator. Nanotechnology, 2006, 17, 5691-5695.	2.6	46
61	Highly selective one-pot synthesis of H-bonded pentagon-shaped circular aromatic pentamers. Chemical Communications, 2011, 47, 5419-5421.	4.1	46
62	Prediction of Water Depth From Multispectral Satellite Imagery—The Regression Kriging Alternative. IEEE Geoscience and Remote Sensing Letters, 2015, 12, 2511-2515.	3.1	46
63	Low-Cost Phase-Selective Organogelators for Rapid Gelation of Crude Oils at Room Temperature. Langmuir, 2016, 32, 13510-13516.	3.5	46
64	Valence-electron distribution inMgB2by accurate diffraction measurements and first-principles calculations. Physical Review B, 2004, 69, .	3.2	44
65	Switching mechanism of photochromic diarylethene derivatives molecular junctions. Journal of Chemical Physics, 2007, 127, 094705.	3.0	44
66	Bathymetry retrieval from optical images with spatially distributed support vector machines. GIScience and Remote Sensing, 2019, 56, 323-337.	5.9	44
67	Efficient organometallic spin filter based on Europium-cyclooctatetraene wire. Journal of Chemical Physics, 2009, 131, .	3.0	43
68	A highly active Pd–P nanoparticle electrocatalyst for enhanced formic acid oxidation synthesized via stepwise electroless deposition. Chemical Communications, 2016, 52, 3556-3559.	4.1	43
69	Magnetism in graphene oxide induced by epoxy groups. Applied Physics Letters, 2015, 106, .	3.3	41
70	Strain effects on point defects and chain-oxygen order-disorder transition in 123 cuprate compounds. Physical Review B, 2004, 70, .	3.2	39
71	Probing the Kinetics of Shortâ€Distance Drug Release from Nanocarriers to Nanoacceptors. Angewandte Chemie - International Edition, 2010, 49, 8426-8430.	13.8	39
72	Structural, Nanomechanical, and Computational Characterization of <scp>d</scp> , <scp>l</scp> -Cyclic Peptide Assemblies. ACS Nano, 2015, 9, 3360-3368.	14.6	39

#	Article	IF	CITATIONS
73	The effects of space charge, dopants, and strain fields on surfaces and grain boundaries in YBCO compounds. Superconductor Science and Technology, 2005, 18, 24-34.	3.5	38
74	Excitons of Edge and Surface Functionalized Graphene Nanoribbons. Journal of Physical Chemistry C, 2010, 114, 17257-17262.	3.1	38
75	The structural and bonding evolution in cysteine–gold cluster complexes. Physical Chemistry Chemical Physics, 2013, 15, 1690-1698.	2.8	38
76	Nanodroplet-Mediated Assembly of Platinum Nanoparticle Rings in Solution. Nano Letters, 2016, 16, 1092-1096.	9.1	38
77	Water permeation dynamics of AqpZ: A tale of two states. Biochimica Et Biophysica Acta - Biomembranes, 2011, 1808, 1581-1586.	2.6	37
78	Chain growth mechanism on bimetallic surfaces for higher alcohol synthesis from syngas. Catalysis Communications, 2015, 61, 57-61.	3.3	37
79	Second-harmonic generation in noncentrosymmetric phosphates. Physical Review B, 2017, 96, .	3.2	37
80	Electronic structure of bilayer graphene: A real-space Green's function study. Physical Review B, 2007, 75, .	3.2	35
81	In vivo studies on non-viral transdifferentiation of liver cells towards pancreatic Î ² cells. Journal of Endocrinology, 2012, 214, 277-288.	2.6	35
82	Enhanced CO2 electroreduction on armchair graphene nanoribbons edge-decorated with copper. Nano Research, 2017, 10, 1641-1650.	10.4	35
83	Plasma density induced formation of nanocrystals in physical vapor deposited carbon films. Carbon, 2011, 49, 1733-1744.	10.3	34
84	Alcohol dehydrogenase-specific T-cell responses are associated with alcohol consumption in patients with alcohol-related cirrhosis. Hepatology, 2013, 58, 314-324.	7.3	33
85	Synthesis, structural investigation and computational modelling of water-binding aquafoldamers. Organic and Biomolecular Chemistry, 2012, 10, 1172-1180.	2.8	32
86	Random Laser With Multiphase-Shifted Bragg Grating in Er/Yb-Codoped Fiber. Journal of Lightwave Technology, 2015, 33, 95-99.	4.6	32
87	Second harmonic generation in the Weyl semimetal TaAs from a quantum kinetic equation. Physical Review B, 2018, 97, .	3.2	32
88	Magnetism in hybrid carbon nanostructures: Nanobuds. Physical Review B, 2009, 79, .	3.2	31
89	Exciton Characteristics in Graphene Epoxide. ACS Nano, 2014, 8, 1284-1289.	14.6	31
90	Synthesis and Characterization of a Series of Annelated Benzotriazole Based Polymers with Variable Bandgap. Journal of Organic Chemistry, 2012, 77, 10035-10041.	3.2	30

#	Article	IF	CITATIONS
91	From benzobisthiadiazole, thiadiazoloquinoxaline to pyrazinoquinoxaline based polymers: effects of aromatic substituents on the performance of organic photovoltaics. Journal of Materials Chemistry, VibrațioRal Spectrum renormalization by enforced coupling across the van der Waals gap	6.7	30
92	between <mml:math xmlns:mml="http://www.w3.org/1998/Math/MathML"><mml:mrow><mml:mi mathvariant="bold">Mo<mml:msub><mml:mi mathvariant="bold">S</mml:mi><mml:mn mathvariant="bold">2</mml:mn </mml:msub></mml:mi </mml:mrow></mml:math> and <mml:math xmlns:mml="http://www.w3.org/1998/Math/MathML"><mml:mrow>and<mml:math< td=""><td>3.2</td><td>30</td></mml:math<></mml:mrow></mml:math 	3.2	30
93	mathvariant="bold">W <mml:msub><mml:mi mathvariant="bold">S</mml:mi><mml:mn mathva Nanoparticulate Contrast Agents for Multimodality Molecular Imaging. Journal of Biomedical Nanotechnology, 2016, 12, 1553-1584.</mml:mn </mml:msub>	1.1	30
94	Human CD4+CD25highCD127low/neg Regulatory T Cells. Methods in Molecular Biology, 2012, 806, 287-299.	0.9	30
95	Impact Ionization and Auger Recombination Rates in Semiconductor Quantum Dots. Journal of Physical Chemistry C, 2010, 114, 3743-3747.	3.1	29
96	Modular peptides from the thermoplastic squid sucker ring teeth form amyloid-like cross-Î ² supramolecular networks. Acta Biomaterialia, 2016, 46, 41-54.	8.3	29
97	Erbium-doped fiber laser with distributed Rayleigh output mirror. Laser Physics, 2014, 24, 115101.	1.2	28
98	Nonlinear electronic polarization and optical response in borophosphate <mml:math xmlns:mml="http://www.w3.org/1998/Math/MathML"><mml:msub><mml:mi>BPO</mml:mi><mml:mn>4Physical Review B, 2016, 93, .</mml:mn></mml:msub></mml:math 	ıl:m s æ/mn	nl:m2 s ub>
99	Algorithmic Foundation and Software Tools for Extracting Shoreline Features from Remote Sensing Imagery and LiDAR Data. Journal of Geographic Information System, 2011, 03, 99-119.	0.5	28
100	Effects of cholesterol on pore formation in lipid bilayers induced by human islet amyloid polypeptide fragments: A coarse-grained molecular dynamics study. Physical Review E, 2011, 84, 051922.	2.1	27
101	Tunable Erbium-Doped Fiber Laser Based on Random Distributed Feedback. IEEE Photonics Journal, 2014, 6, 1-5.	2.0	27
102	Ultrafast Killing and Selfâ€Gelling Antimicrobial Imidazolium Oligomers. Small, 2016, 12, 1928-1934.	10.0	27
103	Role of Water in Catalyzing Proton Transfer in Glucose Dehydration to 5â€Hydroxymethylfurfural. ChemCatChem, 2017, 9, 2784-2789.	3.7	27
104	Cytokine IL-6 is required in Citrobacter rodentium infection-induced intestinal Th17 responses and promotes IL-22 expression in inflammatory bowel disease. Molecular Medicine Reports, 2014, 9, 831-836.	2.4	26
105	NHCâ€Ag/Pdâ€Catalyzed Reductive Carboxylation of Terminal Alkynes with CO ₂ and H ₂ : A Combined Experimental and Computational Study for Fineâ€Tuned Selectivity. ChemSusChem, 2017, 10, 836-841.	6.8	26
106	Quantum Tunneling of Magnetization in Ultrasmall Half-Metallic V3O4 Quantum Dots: Displaying Quantum Superparamagnetic State. Scientific Reports, 2012, 2, 755.	3.3	25
107	Universal Transient Dynamics of Electrowetting Droplets. Scientific Reports, 2018, 8, 836.	3.3	25
108	Electronic, Magnetic, and Transport Properties of Fe-COT Clusters: A Theoretical Study. Journal of Physical Chemistry C, 2010, 114, 11946-11950.	3.1	24

#	Article	IF	CITATIONS
109	Simulations on the effects of confinement and Ni-catalysis on the formation of tubular fullerene structures from peapod precursors. Physical Review B, 2007, 75, .	3.2	23
110	A theoretical study of spin-polarized transport properties of planar four-coordinate Fe complexes. Chemical Physics Letters, 2012, 539-540, 102-106.	2.6	23
111	The acceleration of methanol synthesis and C2 oxygenates formation on copper grain boundary from syngas. Applied Catalysis A: General, 2016, 509, 97-104.	4.3	23
112	Ab initio investigation of Jahn–Teller-distortion-tuned Li-ion migration in λ-MnO ₂ . Journal of Materials Chemistry A, 2017, 5, 9618-9626.	10.3	23
113	Human Leukocyte Antigen Profile Predicts Severity of Autoimmune Liver Disease in Children of European Ancestry. Hepatology, 2021, 74, 2032-2046.	7.3	23
114	Measuring the hole-state anisotropy inMgB2by electron energy-loss spectroscopy. Physical Review B, 2003, 67, .	3.2	22
115	T1846 and A/G1913 are associated with acute on chronic liver failure in patients infected with hepatitis B virus genotypes B and C. Journal of Medical Virology, 2011, 83, 996-1004.	5.0	22
116	Power-referenced refractometer with tilted fiber Bragg grating cascaded by chirped grating. Optics Communications, 2014, 312, 106-109.	2.1	22
117	Magnetic field sensor based on magnetic-fluid-coated long-period fiber grating. Journal of Optics (United Kingdom), 2015, 17, 065402.	2.2	22
118	CTAB-Influenced Electrochemical Dissolution of Silver Dendrites. Langmuir, 2016, 32, 3601-3607.	3.5	22
119	Evaluating the portability of satellite derived chlorophyll-a algorithms for temperate inland lakes using airborne hyperspectral imagery and dense surface observations. Harmful Algae, 2018, 76, 35-46.	4.8	22
120	Reversible metal-insulator transition in LaAlO <mml:math xmlns:mml="http://www.w3.org/1998/Math/MathML" display="inline"><mml:msub><mml:mrow /><mml:mn>3</mml:mn></mml:mrow </mml:msub>thin films mediated by intragap defects: An alternative mechanism for resistive switching. Physical Review B, 2011, 84, .</mml:math 	3.2	21
121	Enhancing magnetic vacancies in semiconductors by strain. Applied Physics Letters, 2012, 100, 072401.	3.3	21
122	Squid Suckerin Biomimetic Peptides Form Amyloid-like Crystals with Robust Mechanical Properties. Biomacromolecules, 2017, 18, 4240-4248.	5.4	21
123	Electronic properties of the coronene series from thermally-assisted-occupation density functional theory. RSC Advances, 2018, 8, 34350-34358.	3.6	21
124	Correlation of EBIC and SWBXT Imaged Defects and Epilayer Growth Pits in 6H-SiC Schottky Diodes. Materials Science Forum, 2000, 338-342, 489-492.	0.3	20
125	Tailoring the Vapor–Liquid–Solid Growth toward the Self-Assembly of GaAs Nanowire Junctions. Nano Letters, 2011, 11, 4947-4952.	9.1	20
126	Theory of high-energy optical conductivity and the role of oxygens in manganites. Physical Review B, 2011, 84, .	3.2	20

#	Article	IF	CITATIONS
127	Comparative studies on the electrochemical and optical properties of representative benzo[1,2-c;4,5-c′]bis[1,2,5]thiadiazole, [1,2,5]-thiadiazolo[3,4-g]quinoxaline and pyrazino[2,3-g]quinoxaline derivatives. Journal of Materials Chemistry C, 2013, 1, 1745.	5.5	20
128	Single quintuple bond [PhCrCrPh] molecule as a possible molecular switch. Journal of Chemical Physics, 2006, 125, 184713.	3.0	19
129	Transport properties through diarylethene derivatives between carbon nanotube electrodes: A theoretical study. Chemical Physics Letters, 2009, 479, 120-124.	2.6	19
130	Molecular Dynamics Simulation Study on the Molecular Structures of the Amylin Fibril Models. Journal of Physical Chemistry B, 2012, 116, 13991-13999.	2.6	19
131	Autoantibody and Human Leukocyte Antigen Profiles in Children With Autoimmune Liver Disease and Their Firstâ€Đegree Relatives. Journal of Pediatric Gastroenterology and Nutrition, 2014, 58, 457-462.	1.8	19
132	Miniature temperature sensor with germania-core optical fiber. Optics Express, 2015, 23, 17687.	3.4	19
133	1â€Chloronaphthaleneâ€Induced Donor/Acceptor Vertical Distribution and Carrier Dynamics Changes in Nonfullerene Organic Solar Cells and the Governed Mechanism. Small Methods, 2022, 6, e2101475.	8.6	19
134	Electronic structure of the antiferromagnetic topological insulator candidate GdBiPt. Physical Review B, 2015, 91, .	3.2	18
135	Theoretical analysis of structures and electronic spectra in molecular cadmium chalcogenide clusters. Journal of Chemical Physics, 2015, 142, 234305.	3.0	18
136	Cuprate-like Electronic Properties in Superlattices with AgIIF2 Square Sheet. Scientific Reports, 2014, 4, 5420.	3.3	18
137	Use of rigid cucurbit[6]uril mediating selective water transport as a potential remedy to improve the permselectivity and durability of reverse osmosis membranes. Journal of Membrane Science, 2021, 623, 119017.	8.2	18
138	Lateral size and thickness dependence in ferroelectric nanostructures formed by localized domain switching. Acta Materialia, 2009, 57, 2047-2054.	7.9	17
139	Scaling of flat band potential and dielectric constant as a function of Ta concentration in Ta-TiO2 epitaxial films. AIP Advances, 2011, 1, 022151.	1.3	17
140	Unzipping carbon nanotubes into nanoribbons upon oxidation: A first-principles study. Nanoscale, 2012, 4, 1254.	5.6	17
141	The transport properties of oxygen vacancy-related polaron-like bound state in HfOx. Scientific Reports, 2013, 3, 3246.	3.3	17
142	A clinicalâ€pathological analysis of hepatitis <scp>B</scp> virus recurrence after liver transplantation in <scp>C</scp> hinese patients. Journal of Gastroenterology and Hepatology (Australia), 2014, 29, 554-560.	2.8	17
143	Color tunable hybrid AC powder electroluminescent devices with organic fluorescent materials. Optical Materials Express, 2016, 6, 2879.	3.0	17
144	New insights into Li diffusion in Li–Si alloys for Si anode materials: role of Si microstructures. Nanoscale, 2019, 11, 14042-14049.	5.6	17

#	Article	IF	CITATIONS
145	Epitaxial engineering of flat silver fluoride cuprate analogs. Physical Review Materials, 2020, 4, .	2.4	17
146	Anomalous polarization switching in organic ferroelectric field effect transistors. Applied Physics Letters, 2007, 91, 042909.	3.3	16
147	Chirally selective growth and extraction of single-wall carbon nanotubes via fullerene nano-peapods. RSC Advances, 2013, 3, 16954.	3.6	16
148	Excitonic Character in Optical Properties of Tetrahedral CdX (X = S, Se, Te) Clusters. Journal of Physical Chemistry C, 2015, 119, 29171-29177.	3.1	16
149	Local Density Approximation for the Short-Range Exchange Free Energy Functional. ACS Omega, 2019, 4, 7675-7683.	3.5	16
150	Manifestation of anisotropy in melting systematics of RBa2Cu3O7â^'δ (R=lanthanides). Applied Physics Letters, 2007, 91, 172510.	3.3	15
151	A novel approach for the design of a highly selective sulfate-ion-selective electrode. Chemical Communications, 2009, , 325-327.	4.1	15
152	Theoretical study on the effective methanol decomposition on Pd(111) surface facilitated in alkaline medium. Journal of Electroanalytical Chemistry, 2011, 662, 251-256.	3.8	15
153	Acid Dissociation of 3-Mercaptopropionic Acid Coated CdSe–CdS/Cd _{0.5} Zn _{0.5} S/ZnS Core–Multishell Quantum Dot and Strong Ionic Interaction with Ca ²⁺ Ion. Journal of Physical Chemistry C, 2016, 120, 3519-3529.	3.1	15
154	The selectivity and activity of catalyst for CO hydrogenation to methanol and hydrocarbon: A comparative study on Cu, Co and Ni surfaces. Surface Science, 2016, 645, 30-40.	1.9	15
155	Momentum distribution and contacts of one-dimensional spinless Fermi gases with an attractive <mml:math xmlns:mml="http://www.w3.org/1998/Math/MathML"><mml:mi>p</mml:mi></mml:math> -wave interaction. Physical Review A, 2018, 98, .	2.5	15
156	Polarization and Electric Field Dependence of Electronic Properties in LaAlO ₃ /SrTiO ₃ Heterostructures. ACS Applied Materials & Interfaces, 2011, 3, 3819-3823.	8.0	14
157	Observation of Frenkel and charge transfer excitons in pentacene single crystals using spectroscopic generalized ellipsometry. Applied Physics Letters, 2013, 103, .	3.3	14
158	GdN thin film: Chern insulating state on square lattice. Physical Review B, 2015, 92, .	3.2	14
159	Electronic Properties of Fluoride and Half–fluoride Superlattices KZnF3/KAgF3 and SrTiO3/KAgF3. Scientific Reports, 2015, 5, 15849.	3.3	14
160	Comparison of satellite reflectance algorithms for estimating turbidity and cyanobacterial concentrations in productive freshwaters using hyperspectral aircraft imagery and dense coincident surface observations. Journal of Great Lakes Research, 2019, 45, 413-433.	1.9	14
161	Non-Catalytic Facile Synthesis of Superhard Phase of Boron Carbide (B ₁₃ C ₂) Nanoflakes and Nanoparticles. Journal of Nanoscience and Nanotechnology, 2012, 12, 596-603.	0.9	13
162	First Principles (DFT) Characterization of Rh ^I /dpppâ€Catalyzed CH Activation by Tandem 1,2â€Addition/1,4â€Rh Shift Reactions of Norbornene to Phenylboronic Acid. Chemistry - A European Journal, 2014, 20, 15625-15634.	3.3	13

#	Article	IF	CITATIONS
163	Mechanistic Study on Oxorheniumâ€Catalyzed Deoxydehydration and Allylic Alcohol Isomerization. Chemistry - an Asian Journal, 2016, 11, 1565-1571.	3.3	13
164	Predicted Weyl fermions in magnetic GdBi and GdSb. International Journal of Modern Physics B, 2017, 31, 1750217.	2.0	13
165	Chiral Pentagon Only Diamond-like Structures. Journal of Physical Chemistry C, 2017, 121, 13810-13815.	3.1	13
166	Optical response of the chiral topological semimetal RhSi. Physical Review B, 2019, 100, .	3.2	13
167	Mechanical properties of sandwich composite made of syntactic foam core and GFRP skins. AIMS Materials Science, 2016, 3, 1704-1727.	1.4	13
168	Substituent effect on the electronic properties of pyrazino[2,3-g] quinoxaline molecules. Journal of Materials Chemistry, 2011, 21, 17798.	6.7	12
169	Ultrafast carrier phonon dynamics in NaOH-reacted graphite oxide film. Applied Physics Letters, 2012, 101, .	3.3	12
170	Synthesis and characterization of three thienopyridazine-based copolymers and their application in OFET. Tetrahedron Letters, 2016, 57, 1523-1527.	1.4	12
171	Electronic mechanism of critical temperature variation inRBa2Cu3O7â^î´. Physical Review B, 2005, 71, .	3.2	11
172	Ballistic Electron Microscopy of Nanographene Layers. Nano Letters, 2008, 8, 4259-4264.	9.1	11
173	Metal-insulator transition at a depleted LaAlO3/SrTiO3 interface: Evidence for charge transfer induced by SrTiO3 phase transitions. Applied Physics Letters, 2011, 99, .	3.3	11
174	Theoretical Modelling and Facile Synthesis of a Highly Active Boronâ€Doped Palladium Catalyst for the Oxygen Reduction Reaction. Angewandte Chemie, 2016, 128, 6956-6961.	2.0	11
175	Opto-impedance spectroscopy and equivalent circuit analyses of AC powder electroluminescent devices. Optics Express, 2017, 25, A454.	3.4	11
176	<mml:math xmlns:mml="http://www.w3.org/1998/Math/MathML"><mml:msub><mml:mi>NaPN</mml:mi><mml:mn>2: Deep-ultraviolet nonlinear optical material with unprecedented strong second-harmonic generation coefficient. Physical Review Materials, 2019, 3, .</mml:mn></mml:msub></mml:math 	nl:mn>2.4	ml:msub>
177	Precise engineering and visualization of signs and magnitudes of DNA writhe on the basis of PNA invasion. Chemical Communications, 2011, 47, 10695.	4.1	10
178	Characteristics of Vδ1+ and Vδ2+ γδT cell subsets in acute liver allograft rejection. Transplant Immunology, 2013, 29, 118-122.	1.2	10
179	Elucidation of thermally induced internal porosity in zinc oxide nanorods. Nano Research, 2018, 11, 2412-2423.	10.4	10
180	Three-Stage Transformation Pathway from Nanodiamonds to Fullerenes. Journal of Physical Chemistry A, 2011, 115, 8327-8334.	2.5	9

HAIBIN SU

#	Article	IF	CITATIONS
181	Molecular Insights into Smallâ€Molecule Drug Discovery for SARSâ€CoVâ€2. Angewandte Chemie, 2021, 133, 9873-9886.	2.0	9
182	Effect of varying the TD-lc-DFTB range-separation parameter on charge and energy transfer in a model pentacene/buckminsterfullerene heterojunction. Journal of Chemical Physics, 2021, 154, 054102.	3.0	9
183	One-Minute Synthesis via Electroless Reduction of Amorphous Phosphorus-Doped Graphene for Oxygen Reduction Reaction. ACS Applied Energy Materials, 2021, 4, 5388-5391.	5.1	9
184	Computational Investigation of the 1,4â€Rh Shift in the [(Ph ₂ PCH ₂ CH ₂ Ph ₂)Rh] atalyzed Alkyne Arylation Reaction. European Journal of Organic Chemistry, 2015, 2015, 7114-7121.	2.4	8
185	Significance of monitoring plasma concentration of voriconazole in a patient with liver failure. Medicine (United States), 2017, 96, e8039.	1.0	8
186	Structural design of microbicidal cationic oligomers and their synergistic interaction with azoles against Candida albicans. Scientific Reports, 2019, 9, 11885.	3.3	8
187	PhaseTransformations in the High-Tc Superconducting Compounds, Ba2RCu3O7-delta (R = Nd, Sm, Gd, Y,) Tj ET	Qq110.7	'84314 rgBT
188	Kagome antiferromagnet: A Schwinger-boson mean-field theory study. Physical Review B, 2007, 76, .	3.2	7
189	Effects of Forward Body Bias on High-Frequency Noise in 0.18-\$mu{hbox{m}}\$ CMOS Transistors. IEEE Transactions on Microwave Theory and Techniques, 2009, 57, 972-979.	4.6	7
190	A novel data selection method based on shadowed sets. Procedia Engineering, 2011, 15, 1410-1415.	1.2	7
191	Locking high energy 1D chain of dichloromethane molecules containing abnormally short Clâ< [–] Cl contacts of 2.524 A inside organic crystals. Organic and Biomolecular Chemistry, 2012, 10, 5525.	2.8	7
192	Population Shift between the Open and Closed States Changes the Water Permeability of an Aquaporin Z Mutant. Biophysical Journal, 2012, 103, 212-218.	0.5	7
193	Dissimilar stability of proteins in graphene bilayer: a molecular dynamics study. Molecular Physics, 2013, 111, 545-552.	1.7	7
194	Comparative Studies on Rigid Ï€ Linkerâ€Based Organic Dyes: Structure–Property Relationships and Photovoltaic Performance. ChemSusChem, 2014, 7, 3396-3406.	6.8	7
195	Interface-induced magnetic coupling in multiferroic/ferromagnetic bilayer: An ultrafast pump-probe study. Applied Physics Letters, 2014, 104, 141602.	3.3	7
196	Formation of "A-frame―dirhenium(I) hexacarbonyl complexes by trans -1,2-bis(diphenylphosphino)ethylene and bis(bidentate) ligands. Journal of Organometallic Chemistry, 2015, 792, 211-219.	1.8	7
197	Dielectric relaxation in AC powder electroluminescent devices. Solid State Communications, 2017, 250, 53-56.	1.9	7
198	Anomalous Photoinduced Reconstructing and Dark Self-Healing Processes on Bi ₂ O ₂ S Nanoplates. Journal of Physical Chemistry Letters, 2020, 11, 7832-7838.	4.6	7

#	Article	IF	CITATIONS
199	A Integrated Map Matching Algorithm Based on Fuzzy Theory for Vehicle Navigation System. , 2006, , .		6
200	Orbital-dependent Electron-Hole Interaction in Graphene and Associated Multi-Layer Structures. Scientific Reports, 2015, 5, 17337.	3.3	6
201	Be12O12 Nano-cage as a Promising Catalyst for CO2 Hydrogenation. Scientific Reports, 2017, 7, 40562.	3.3	6
202	Identifying Different Spin Mixing Channels Occurring in Charge-Transfer States. Journal of Physical Chemistry C, 2020, 124, 14832-14837.	3.1	6
203	Optical detection of quantum geometric tensor in intrinsic semiconductors. Science China: Physics, Mechanics and Astronomy, 2021, 64, 1.	5.1	6
204	Orbital-adapted electronic structure and anisotropic transport in <mml:math xmlns:mml="http://www.w3.org/1998/Math/MathML"><mml:mrow><mml:mi>l³</mml:mi><mml:mtext>â^'mathvariant="normal">O<mml:mn>3</mml:mn><mml:mo>/</mml:mo><mml:msub><n heterostructure. Physical Review Materials, 2020, 4, .</n </mml:msub></mml:mtext></mml:mrow></mml:math 	nl:mtext> nml:mi>Sr	<mml:msub>< TiO</mml:msub>
205	A adaptive map matching algorithm based on Fuzzy-Neural-Network for vehicle navigation system. , 2008, , .		5
206	Recognition of forcible curvature in circular DNA by human topoisomerase I. Chemical Communications, 2011, 47, 11309.	4.1	5
207	Magnetism in Thiolated Gold Model Junctions. Journal of Physical Chemistry C, 2012, 116, 17714-17720.	3.1	5
208	Investigation of work function and surface energy of aluminum: An ab-initio study. , 2013, , .		5
209	The mechanism of transforming diamond nanowires to carbon nanostructures. Nanotechnology, 2014, 25, 035601.	2.6	5
210	Method to extract multiple states in F ₁ -ATPase rotation experiments from jump distributions. Proceedings of the National Academy of Sciences of the United States of America, 2019, 116, 25456-25461.	7.1	5
211	Unraveling Dynamic Transitions in Time-Resolved Biomolecular Motions by A Dressed Diffusion Model. Journal of Physical Chemistry A, 2020, 124, 613-617.	2.5	5
212	New biosensors made of specially designed transparent chips with nano-optical tags. Smart Materials and Structures, 2007, 16, 2214-2221.	3.5	4
213	Incommensurate phase of a triangular frustrated Heisenberg model studied via Schwinger-boson mean-field theory. Journal of Physics Condensed Matter, 2009, 21, 326005.	1.8	4
214	A graph-based approach for assessing storm-induced coastal changes. International Journal of Remote Sensing, 2016, 37, 4854-4873.	2.9	4
215	Electrical and electrochemical properties of triphenylene based lithium solvated electron solutions. Electrochimica Acta, 2018, 292, 142-146.	5.2	4
216	Supramolecular Protein Assembly Retains Its Structural Integrity at Liquid–Liquid Interface. Advanced Materials Interfaces, 2020, 7, 1901674.	3.7	4

#	Article	IF	CITATIONS
217	SOFT X-RAY ABSORPTION SPECTROSCOPY OF THE MgB2 BORON K EDGE IN AN MgB2/Mg COMPOSITE. Modern Physics Letters B, 2006, 20, 1207-1216.	1.9	3
218	Pair-Hopping Characteristic of Lithium Diffusive Motion in Li-Doped Î ² -Phase Manganese Phthalocyanine. Journal of Physical Chemistry B, 2007, 111, 10064-10068.	2.6	3
219	ELECTRONIC AND STERIC MECHANISMS IN MONO- AND DOUBLE-FLUORINATION OF Cs-C60Cl6. Modern Physics Letters B, 2008, 22, 2727-2738.	1.9	3
220	Weyl Ordering Symbol Method for Studying Wigner Function of the Damping Field. International Journal of Theoretical Physics, 2010, 49, 2016-2027.	1.2	3
221	Vibrational excitations in molecular layers probed by ballistic electron microscopy. Nanotechnology, 2011, 22, 435701.	2.6	3
222	Robust dynamical compensator design for discrete-time linear periodic systems. Journal of Global Optimization, 2012, 52, 291-304.	1.8	3
223	Electronic reconstruction and surface two-dimensional electron gas in a polarized heterostructure with a hole-doped single copper-oxygen plane. Physical Review B, 2013, 87, .	3.2	3
224	Phase Diagram of Solid-Phase Transformation in Amorphous Carbon Nanorods. Journal of Physical Chemistry A, 2014, 118, 9163-9172.	2.5	3
225	Fractional Mott insulator-to-superfluid transition of Bose–Hubbard model in a trimerized Kagomé optical lattice. Journal of Physics Condensed Matter, 2016, 28, 256001.	1.8	3
226	Theoretical Modeling, Facile Fabrication, and Experimental Study of Optimally Bound Bilirubin Oxidase on Palladium Nanoparticles for Enhanced Oxygen Reduction Reaction. ACS Catalysis, 2018, 8, 4950-4954.	11.2	3
227	Coupled Mutations-Enabled Glycerol Transportation in an Aquaporin Z Mutant. ACS Omega, 2018, 3, 4113-4122.	3.5	3
228	Stratification Modelling of Key Bacterial Taxa Driven by Metabolic Dynamics in Meromictic Lakes. Scientific Reports, 2018, 8, 9538.	3.3	3
229	Generalization of Langevin Dynamics from Spatio-Temporal Dressed Dynamics Perspective. Journal of Physical Chemistry A, 2020, 124, 3269-3275.	2.5	3
230	Publisher's Note: Average density of states in disordered graphene systems [Phys. Rev. B 77 , 195411 (2008)]. Physical Review B, 2008, 77, .	3.2	2
231	Ab initio simulation of electronic and mechanical properties of aluminium for fatigue early feature investigation. International Journal of Nanotechnology, 2014, 11, 373.	0.2	2
232	Highly sensitive magnetic field sensor using long-period fiber grating. , 2015, , .		2
233	Band topologies of hexaborides CaB6 and EuB6. Science China: Physics, Mechanics and Astronomy, 2017, 60, 1.	5.1	2
234	Electrochemical Properties of Anthracene-Based Lithium-Solvated Electron Solutions. ACS Omega, 2019, 4, 4707-4711.	3.5	2

HAIBIN SU

#	Article	IF	CITATIONS
235	Contrasting Historical and Recent Breakup Styles on the Meade River of Arctic Alaska in the Context of a Warming Climate. American Journal of Climate Change, 2013, 02, 165-172.	0.9	2
236	POLARIZABILITY AND SHIELDING OF COAXIAL HYBRID DOUBLE-WALLED NANOTUBES: A FIRST-PRINCIPLES STUDY. Journal of Theoretical and Computational Chemistry, 2008, 07, 793-803.	1.8	1
237	Transverse dispersion and interfacial dephasing effects on the shape and amplitude of the ballistic-electron-emission spectroscopy of nanographenes. Journal of Physics Condensed Matter, 2012, 24, 255303.	1.8	1
238	Supramolecular Assemblies: Supramolecular Protein Assembly Retains Its Structural Integrity at Liquid–Liquid Interface (Adv. Mater. Interfaces 4/2020). Advanced Materials Interfaces, 2020, 7, 2070021.	3.7	1
239	Electrochemical properties of p-terphenyl based lithium solvated electron solutions. Journal of Electroanalytical Chemistry, 2020, 875, 114148.	3.8	1
240	On fractional charge in molecules and materials. Theoretical Chemistry Accounts, 2020, 139, 1.	1.4	1
241	Mechanisms of Efficient Desalination by a Two-Dimensional Porous Nanosheet Prepared via Bottom-Up Assembly of Cucurbit[6]urils. Membranes, 2022, 12, 252.	3.0	1
242	Gauche Effect on 2D Phosphorus Allotropes' Energetics. Journal of Physical Chemistry C, 2022, 126, 8883-8888.	3.1	1
243	NOVEL NANO-DEVICE ANDSYMMETRYROLE IN CHEMICAL EVENT OF C60 AND CARBON NANOTUBE COMPOSITE. , 2008, , .		0
244	Travel time estimating algorithms based on Fuzzy Radial Basis Function Neural Networks. , 2010, , .		0
245	Reply to "Comment on 'Impact Ionization and Auger Recombination Rates in Semiconductor Quantum Dots'― Journal of Physical Chemistry C, 2010, 114, 16860-16860.	3.1	0
246	Nanodiamond clusters and their tranformation into fullerene at high temperature: A tight-binding simulation. , 2010, , .		0
247	A Maximum Power Point Tracking Algorithm Based on Fuzzy Neural Networks for Grid-Connected Photovoltaic System. Advanced Materials Research, 0, 291-294, 2771-2774.	0.3	0
248	Evaluation of Vehicle Combination Property Based on Evidential Reasoning Method. Advanced Materials Research, 0, 433-440, 5142-5146.	0.3	0
249	Multi-paradigm simulation at nanoscale: Methodology and application to functional carbon material. , 2012, , .		0
250	Frontispiz: Theoretical Modelling and Facile Synthesis of a Highly Active Boron-Doped Palladium Catalyst for the Oxygen Reduction Reaction. Angewandte Chemie, 2016, 128, .	2.0	0
251	Frontispiece: Theoretical Modelling and Facile Synthesis of a Highly Active Boron-Doped Palladium Catalyst for the Oxygen Reduction Reaction. Angewandte Chemie - International Edition, 2016, 55, .	13.8	0
252	Computation-guided improved one-pot synthesis of macrocyclic cation-binding aromatic pyridone pentamers. Organic and Biomolecular Chemistry, 2016, 14, 9961-9965.	2.8	0

#	Article	IF	CITATIONS
253	Mid-infrared supercontinuum generation by nanosecond diode pumping. , 2017, , .		0
254	Structural evolution dynamics in fusion of sumanenes and corannulenes: defects formation and self-healing mechanism. Nano Futures, 2018, 2, 025001.	2.2	0
255	Mid-infrared Raman sources with highly GeO2-doped silica optical fibers. , 2015, , .		0
256	Optical-field induced SU(2) pair potential in caesium lead halide perovskites. International Journal of Modern Physics B, 2021, 35, 2150030.	2.0	0